

Magnetic properties of $\text{Fe}_{0.9-q}\text{Mn}_{0.1}\text{Al}_q$ disordered alloys: Theory

J. Restrepo and G. A. Pérez Alcázar

Departamento de Física, Universidad del Valle, AA 25360, Cali, Colombia

(Received 20 September 1999)

By using the free-energy variational method based on the Bogoliubov inequality and a diluted and random-bond Ising model with nearest-neighbors interactions, we investigate the magnetic phase diagram and some of the magnetic properties of the disordered $\text{Fe}_{0.9-q}\text{Mn}_{0.1}\text{Al}_q$ alloys system. Thus the mean magnetization per site, and hence the average hyperfine magnetic field, are computed. The so-obtained results are compared with room-temperature experimental data obtained by ^{57}Fe Mössbauer spectroscopy and vibrating sample magnetometry, from which a very good agreement is achieved. Here, the occurrence of a “critical concentration” at 40.0 at. % Al, for which the system passes from a ferromagnetically ordered state to a paramagnetic one, is evidenced. The model allows obtaining an estimate of the exchange energy between Fe-Fe pairs. How this energy depends on the Al concentration and the role of the manganese atoms is also presented and discussed.

The FeMnAl alloys system is beginning to acquire a great interest thanks to many of its mechanical and magnetic properties and the possibility to be applied as a stainless steel and as a semisoft magnetic material.¹ An enormous interest has also arisen from both the experimental and theoretical points of view to study the spin glass and the reentrant spin-glass behaviors, which are present in these sorts of alloys.²⁻⁴ The origin of such behaviors is motivated by the occurrence of several ingredients like competitive interactions, dilution, and disorder. However, the works reported on the literature,²⁻⁶ dealing with magnetic properties of disordered FeMnAl alloys, correspond to some few series in composition of the structural phase diagram. Thus the contribution of the present work is the study of a series with 10 at. % Mn constant, in which a theoretical interpretation of previous experimental results⁷ is carried out. The framework of such interpretation is the variational principle for the free energy of a thermodynamic system based on the Bogoliubov inequality.^{8,9} The method is also implemented with an Ising model involving nearest neighbors interactions, and a probability function to account for a distribution of atomic configurations linked to the disorder.

In the present work we present theoretical results of the magnetic properties corresponding to the $\text{Fe}_{0.9-q}\text{Mn}_{0.1}\text{Al}_q$ alloy series with $0.1 \leq q \leq 0.5$. The Al concentration dependence of the average hyperfine magnetic field and the magnetization is investigated and compared with experimental results⁷ obtained by means of Mössbauer spectroscopy and vibrating sample magnetometry. Finally, the model allows obtaining estimates of the exchange energies for the different types of bonds present in the system.

Samples, from which the experimental results were obtained,⁷ were prepared by following the Chakrabarti method,¹⁰ in which the disorder was achieved through high temperature and quenching. Such experimental results⁷ consisted on measurements of ^{57}Fe Mössbauer spectroscopy, vibrating sample magnetometry (VSM), and x-ray (Cu, $K\alpha$) diffraction. Mössbauer spectra were fitted, according to the disordered character of the samples, with hyperfine field dis-

tributions. VSM measurements were carried out in a Foner-type magnetometer with a maximum external applied field of 8.2 kOe.

The variational approach based on the Bogoliubov inequality^{8,9} is a helpful method to compute the free energy and thermodynamic properties of a given system. It proposes that

$$F \leq \Phi(\gamma) \equiv [F_0(\gamma)] + [\langle H - H_0(\gamma) \rangle_0], \quad (1)$$

where F is the free energy defined by an exact Hamiltonian H , F_0 is the free energy linked to the trial Hamiltonian $H_0(\gamma)$, γ represents a set of variational parameters, $\langle \dots \rangle_0$ means thermal average in the ensemble defined by H_0 , and $[\dots]$ is the configurational average taken over the distribution of all possible configurations in the disordered system according to the following proposed probability function:

$$P(J_{ij}) = p^2 \delta(J_{ij} - J) + x^2 \delta(J_{ij} + \lambda J) + 2px \delta(J_{ij} + \alpha J) + (q^2 + 2pq + 2qx) \delta(J_{ij}), \quad (2)$$

where p^2 represents the probability of having two nearest Fe neighbors interacting ferromagnetically with an exchange energy of strength J , analogously, x^2 is the probability for an antiferromagnetic Mn-Mn pair with energy $-\lambda J$, $2px$ the probability for an antiferromagnetic Fe-Mn pair with energy $-\alpha J$, and the last term represents the probability of having nonmagnetic diluted bonds involving Al (Al-Al, Fe-Al, and Mn-Al). p , x , and q represent the fractional concentrations of Fe, Mn, and Al, respectively, obeying the relationship $p + x + q = 1$.

As the exact Hamiltonian H , we have chosen an Ising one with nearest neighbors interactions:

$$H = - \sum_{\langle i,j \rangle} J_{ij} \sigma_i \sigma_j, \quad (3)$$

where the sum runs over nearest neighbors and $\sigma_i = \pm 1$. The trial Hamiltonian was taken to be⁹

$$H_0 = -\gamma_s \sum_i^{n_1} \sigma_i - \sum_{\substack{\{j,k\} \\ j \neq k}}^{2n_2} J_{jk} \sigma_j \sigma_k - \gamma_p \sum_j^{2n_2} \sigma_j. \quad (4)$$

Here, the system is considered as formed by n_1 isolated spins and n_2 linked pairs, so that the total number of spins N is given by

$$N = n_1 + 2n_2. \quad (5)$$

Thus the first sum in Eq. (4) extends over n_1 isolated spins, and the sum in the last two terms extends over $2n_2$ spins belonging to linked pairs. γ_s and γ_p are two variational parameters, representing molecular fields, to be determined from the following two conditions: (i) the value of Φ , given by Eq. (1), must be minimized, and (ii) the magnetization per site $m \equiv [\langle \sigma_i \rangle]$ is the same regardless whether the spin σ_i is isolated or it belongs to a linked pair.

Now we can write for the free energy F_0 the following expression:

$$F_0 = -\frac{1}{\beta} \ln Z_0 = -k_B T \ln(Z_s^{N-2n_2} Z_p^{n_2}), \quad (6)$$

where

$$Z_0 = \sum_{\{\sigma\}} \exp(-\beta H_0) \quad (7)$$

and

$$Z_s = 2 \cosh(\beta \gamma_s), \quad (8)$$

$$Z_p = 2e^{\beta J_{ij}} \cosh(2\beta \gamma_p) + 2e^{-\beta J_{ij}} \quad (9)$$

are the trial partition functions for isolated and linked spins pairs, respectively. And $\beta = (k_B T)^{-1}$. The configurational average of F_0 , to be replaced in Eq. (1), is calculated from

$$[F_0] = \int F_0 P(J_{ij}) dJ_{ij}. \quad (10)$$

By using the distribution function given by Eq. (2), we get

$$\begin{aligned} [F_0] = & -k_B T (N - 2n_2) \ln Z_s - n_2 k_B T \{ p^2 \ln Z_p(J) \\ & + x^2 \ln Z_p(-\lambda J) + 2px \ln Z_p(-\alpha J) \\ & + (q^2 + 2pq + 2qx) \ln Z_p(0) \}. \end{aligned} \quad (11)$$

For the thermal average $\langle H - H_0(\gamma) \rangle_0$, we obtain

$$\begin{aligned} \langle H - H_0(\gamma_s, \gamma_p) \rangle_0 = & -J_{ij} m^2 \left(\frac{Nz}{2} - n_2 \right) + (N - 2n_2) \gamma_s m \\ & + 2n_2 \gamma_p m, \end{aligned} \quad (12)$$

where z is the coordination number ($z=8$ for a bcc lattice), and where we have assumed that the spins are statistically independent, so that $\langle \sigma_j \sigma_k \rangle = m^2$. By doing the configurational average over Eq. (12), we obtain

$$\begin{aligned} [\langle H - H_0 \rangle_0] = & - \left(\frac{Nz}{2} - n_2 \right) (p^2 - \lambda x^2 - 2\alpha p x) J m^2 \\ & + (N - 2n_2) \gamma_s m + 2n_2 \gamma_p m. \end{aligned} \quad (13)$$

Hence the total energy $\Phi(\gamma_s, \gamma_p)$ of the system would be the sum of Eqs. (11) and (13) according to Eq. (1). A minimization of Φ with respect to m leads to the following relation between the molecular fields:

$$\gamma_s = \left(\frac{z}{z-1} \right) \gamma_p, \quad (14)$$

where we have chosen $n_2 = Nz/2$, which corresponds to the maximum number of bonds we can obtain from a lattice with N spins. This choice for n_2 is also motivated by the fact that Φ decreases monotonically as n_2 increases. Thus in order to get the best approach in the minimization process of the free energy, n_2 has to be as large as physically possible.

On the other hand, as we have already mentioned, $m \equiv [\langle \sigma_i \rangle]$, can be obtained either for an isolated spin or for a spin belonging to a linked pair, so we have

$$m = \left[\frac{1}{\beta} \frac{\partial \ln Z_s}{\partial \gamma_s} \right] = \left[\frac{1}{2\beta} \frac{\partial \ln Z_p}{\partial \gamma_p} \right], \quad (15)$$

from which we finally get the following relationship for the magnetization per site:

$$\begin{aligned} m = & \tanh(\beta \gamma_s) \\ = & \sinh(2\beta \gamma_p) \left\{ \frac{p^2}{\cosh(2\beta \gamma_p) + e^{-2\beta J}} \right. \\ & + \frac{x^2}{\cosh(2\beta \gamma_p) + e^{2\beta \lambda J}} + \frac{2px}{\cosh(2\beta \gamma_p) + e^{2\beta \alpha J}} \\ & \left. + \frac{q^2 + 2pq + 2qx}{\cosh(2\beta \gamma_p) + 1} \right\}, \end{aligned} \quad (16)$$

where γ_s and γ_p are related through Eq. (14). The roots of Eq. (16) were computed by using the Newton-Raphson method.

The calculation of the critical temperature T_c from Eq. (16), for which $m=0$, leads to the following expression:

$$\begin{aligned} \frac{z}{2(z-1)} = & \frac{p^2}{1 + e^{-2\beta_c J}} + \frac{x^2}{1 + e^{2\beta_c \lambda J}} + \frac{2px}{1 + e^{2\beta_c \alpha J}} \\ & + \frac{q^2 + 2pq + 2qx}{2}, \end{aligned} \quad (17)$$

where $\beta_c = (k_B T_c)^{-1}$. From this equation, the magnetic phase diagram was computed.

Now, if we assume that the average hyperfine magnetic field $\langle H \rangle$ is directly proportional to the magnetization m , it is then reasonable to propose the following relationship:^{6,11}

$$\langle H(q, T) \rangle = \wp m(q, T), \quad (18)$$

where \wp is a constant of proportionality. Hence we get

$$\frac{\langle H(q, T) \rangle}{\langle H(0.1, RT) \rangle} = \frac{m(q, T)}{m(0.1, RT)}, \quad (19)$$

where $\langle H(q, T) \rangle$ is the average hyperfine field at temperature T and Al content q ; $\langle H(0.1, RT) \rangle = 26.0 \pm 1.0$ T is the average hyperfine field at room temperature ($RT = 295$ K) and 10 at. % Al. This last value, corresponding to the $\text{Fe}_{0.9}\text{Mn}_{0.1}\text{Al}_{0.1}$ alloy, was obtained from the experimental data,⁷ and the reason for considering it as normalization factor instead of

$\langle H(0,RT) \rangle$ for $q=0$, is because for Al concentrations below 10 at. %, the system undergoes a martensite transformation as is known from the structural phase diagram.¹⁰ Analogously, $m(q,T)$ and $m(0.1,RT)$, to be obtained from Eq. (16), correspond to the magnetization per site at temperature T , Al content q , and at room temperature and 10 at. % Al, respectively.

Similarly, since the bulk magnetization M is assumed to be proportional to the magnetization per site m , these quantities should be related according to

$$\frac{M(q,T)}{M(0.1,RT)} = \frac{m(q,T)}{m(0.1,RT)}, \quad (20)$$

where $M(0.1,RT) = 150 \pm 10$ emu/g obtained from the experimental results,⁷ is the saturation magnetization at room temperature and $q=0.1$.

By comparing Eqs. (19) and (20) we observe that they have exactly the same mathematical form, which indicates both the bulk magnetization and the average hyperfine field must obey the same scale relation as one expects.

Finally, in order to take into account the effect of the increment of the lattice parameter upon the exchange energy as the Al concentration is increased, which has been already verified through x-ray-diffraction measurements,^{6,11-13} due to the larger atomic size of the Al atoms, we have used the following relationship, in a first-order approach, for the exchange energy:^{6,11-13}

$$J = J(q) = J_1 - J_0 q, \quad (21)$$

where J_1 and J_0 are parameters to be adjusted based on the experimental results. This expression has been already used for bcc FeAl (Refs. 11-13) and fcc FeMnAl (Ref. 6) disordered alloys, in which the lattice expansion effect due to aluminum, dealing with a reduction in the exchange energy has been already verified and analyzed.

As is reported in Ref. 7, x-ray-diffraction measurements revealed a body-centered-cubic (bcc) structure in the whole-considered Al concentration range. Also, as the Al content was increased, the lattice parameter increased from 2.890 up to 2.960 ± 0.005 Å in a close linear fashion.¹ Thus our system behaves, from the structural point of view, as the disordered bcc FeAl system does,¹¹ for which the expression (21) was successfully used to interpret the magnetic properties of that system.

Figure 1 shows the theoretical magnetic phase diagram obtained from Eq. (17), in which the Curie temperature decreases monotonically as the Al concentration is increased. This behavior agrees with the nonmagnetic character of the Al atoms, which are responsible for the dilution between ferromagnetically coupled Fe-Fe bonds. The values we used in Eq. (17) for J_1 and J_0 in order to determine J in Eq. (21) were fitted accordingly with the experimental results,⁷ which reveal a magnetic phase transition from a ferromagnetic state to a paramagnetic one at room temperature (295 K) and 40.0 at. % Al (Fig. 2). The best choice of these parameters was $J_1 = 19.0$ meV, giving the strength of the ferromagnetic Fe-Fe bond ($J = J_1 = J_{\text{Fe-Fe}}$ for $q=0$), and $J_0 = 0.33J_1$, which means that the exchange energy $J_{\text{Fe-Fe}}$ is reduced in a 33% per concentration unit of the dilutor element (Al). Analogously, in order to get the best fit, the choice of the param-

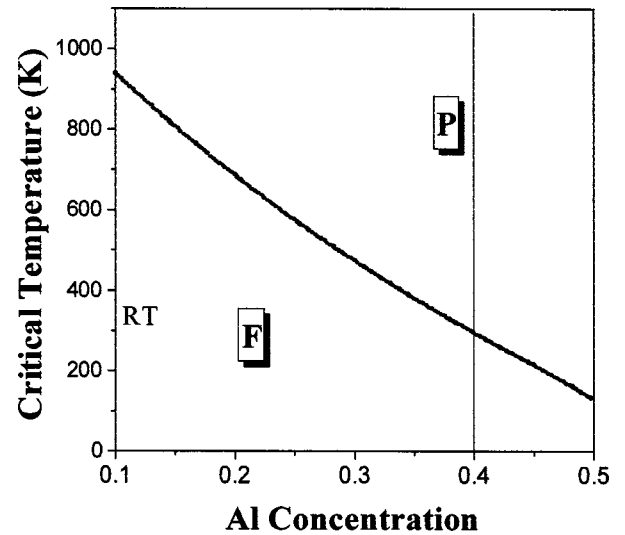


FIG. 1. Magnetic phase diagram for $\text{Fe}_{0.9-q}\text{Mn}_{0.1}\text{Al}_q$ disordered alloys, obtained from Eq. (17). ‘‘F’’ and ‘‘P’’ denote the ferromagnetic and paramagnetic phases, respectively.

eters λ and α , accounting for the Mn-Mn and Fe-Mn interactions, respectively, gave both a zero value. This result seems to be surprising but is not; it is interpreted by saying that the strength of the bond energies between Mn-Mn and Fe-Mn moments is much smaller than the corresponding Fe-Fe pairs, i.e., $J_{\text{Mn-Mn}} \ll J_{\text{Fe-Fe}}$ and $J_{\text{Fe-Mn}} \ll J_{\text{Fe-Fe}}$. This feature seems to be reasonable since our system is an iron-rich system involving a ferromagnetic matrix in which the Fe atoms are supposed to be strongly ferromagnetically coupled to their nearest Fe neighbors.

In addition, the result is in agreement with the values $\alpha = 0.005$ ($J_{\text{Fe-Mn}} = 0.5\% J_{\text{Fe-Fe}}$) and $\lambda = 0.03$ ($J_{\text{Mn-Mn}} = 3\% J_{\text{Fe-Fe}}$), reported for $\text{Fe}_{0.7-x}\text{Mn}_x\text{Al}_{0.3}$ disordered alloys.⁵ The small values obtained for J_{FeMn} and J_{MnMn} are also in agreement with the prediction of Rosales Rivera

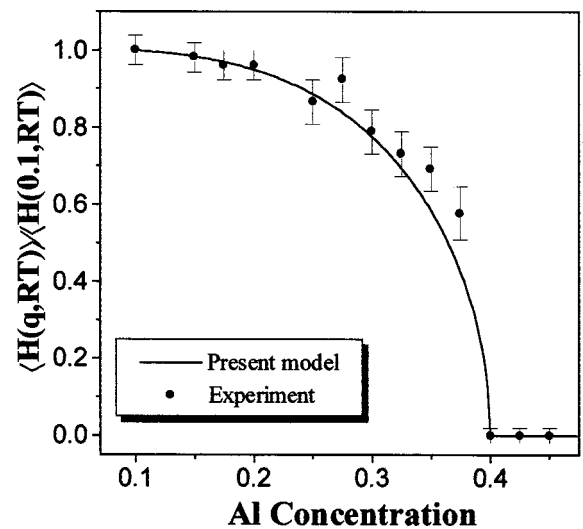


FIG. 2. Al content dependence of the reduced average hyperfine magnetic field of disordered $\text{Fe}_{0.9-q}\text{Mn}_{0.1}\text{Al}_q$ alloys at room temperature (295 K). Solid circles correspond to the experimental data obtained by Mössbauer, and the solid line corresponds to the theoretical results predicted by the present model.

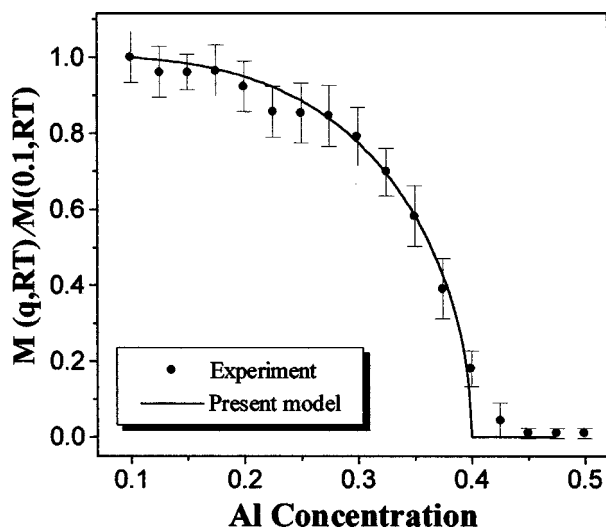


FIG. 3. Al concentration dependence of the reduced bulk magnetization at 8.2 kOe of disordered $\text{Fe}_{0.9-q}\text{Mn}_{0.1}\text{Al}_q$ alloys at room temperature (295 K). Solid circles correspond to the experimental data obtained by vibrating sample magnetometry, and the solid line corresponds to the theoretical results predicted by the present model.

et al.,¹⁵ who obtained that the antiferromagnetic couplings are smaller for low Mn contents (as in this work) and they increase as the Mn concentration increases. The value of 19 meV obtained for the exchange energy between iron pairs is also within the range reported (10–50 meV) for FeNi and FeCo alloys,¹⁴ and it is also in very good agreement with that reported (23 meV) in $\text{Fe}_{0.7-x}\text{Mn}_x\text{Al}_{0.3}$ disordered alloys.⁵

Figure 2 shows both the experimental and theoretical reduced average hyperfine field as a function of the Al content at room temperature. The experimental data were obtained by fitting the Mössbauer spectra,⁷ and the theoretical ones were obtained by using Eqs. (16), (19), and (21) with the above given numerical results. As it can be observed, the fitted parameters give rise to a good agreement between experiment and theory. However a small discrepancy arises as the Al concentration is approached to 40 at. %. Such difference, in which the predicted data are systematically below

the experimental ones, can be attributed to the limitation of our model, which only takes into account nearest-neighbors interactions. In addition, due to the disordered character of the system, other contributions to the average hyperfine field coming from larger clusters (involving, for instance, second and third nearest neighbors) can take place.

The well behaved decrease in the average hyperfine field as the Al concentration is increased (Fig. 2) can be ascribed to the nonmagnetic character of the Al atoms and their capability of breaking up magnetic bonds. This dilution process give rise to the occurrence of a “critical concentration” q_c above which the system loses its long-range ferromagnetic order and becomes paramagnetic. Below q_c what we have are distributions of clusters giving nonzero contributions to the bulk magnetization of the system, which is considered as proportional to the average hyperfine field according to Eq. (18), and q_c might be then interpreted as that concentration for which a bond percolation phenomenon is established.

Figure 3 shows both the experimental and theoretical reduced bulk magnetization as a function of the Al content at room temperature. The experimental data correspond to the reduced bulk specific magnetization at 8.2 kOe, and they were obtained from hysteresis loops, which were measured in a vibrating sample magnetometer.⁷ The theoretical curve was obtained by using Eqs. (16), (20), and (21) with the same choice of parameters as was carried out for the computation of the average hyperfine field.

As the critical Al concentration (40 at. %) is approached, the magnetization drops rapidly to small values, which seems to be correlated with the paramagnetic behavior obtained by Mössbauer as well as with the predicted one.

We conclude according to the obtained results, for which a very well agreement between theory and experiment was achieved, that the present model seems to be a suitable model in the study of the magnetic properties of $\text{Fe}_{0.9-q}\text{Mn}_{0.1}\text{Al}_q$ disordered alloys.

The authors would like to express their gratitude to COLCIENCIAS, Colombian Agency for the Scientific Development, and Universidad del Valle, for their financial support.

¹J. Restrepo, G. A. Pérez Alcázar, and J. M. González, *Hyperfine Interact.* (to be published).

²H. Bremers, Ch. Jarms, J. Hesse, S. Chadjivasilou, K. G. Efthimiadis, and I. Tsoukalas, *J. Magn. Magn. Mater.* **63**, 140 (1995).

³G. A. Pérez Alcázar, Ligia E. Zamora, A. Bohórquez, E. González, and J. M. González, *J. Appl. Phys.* **79**, 6155 (1996).

⁴Ligia E. Zamora, G. A. Pérez Alcázar, A. Bohórquez, and J. A. Tabares, *J. Magn. Magn. Mater.* **137**, 339 (1994).

⁵Ligia E. Zamora, G. A. Pérez Alcázar, A. Bohórquez, J. F. Marco, and J. M. González, *J. Appl. Phys.* **82**, 6165 (1997).

⁶A. Osorio, Ligia E. Zamora, and G. A. Pérez Alcázar, *Phys. Rev. B* **53**, 8176 (1996).

⁷J. Restrepo, G. A. Pérez Alcázar, and J. M. González (unpub-

lished).

⁸H. Falk, *Am. J. Phys.* **38**, 858 (1970).

⁹L. G. Ferreira, S. R. Salinas, and M. J. Oliveira, *Phys. Status Solidi B* **83**, 229 (1977).

¹⁰D. J. Chakrabarti, *Metall. Trans. B* **8**, 121 (1977).

¹¹G. A. Pérez Alcázar, J. A. Plascak, and E. Galvao da Silva, *Phys. Rev. B* **34**, 1940 (1986).

¹²J. Restrepo, G. A. Pérez Alcázar, and J. M. González, *J. Appl. Phys.* **83**, 7249 (1998).

¹³J. Restrepo, J. M. González, and G. A. Pérez Alcázar, *J. Appl. Phys.* **81**, 5270 (1997).

¹⁴S. N. Kaul, *Phys. Rev. B* **27**, 5761 (1983).

¹⁵A. Rosales Rivera, G. A. Pérez Alcázar, and J. A. Plascak, *Phys. Rev. B* **41**, 4774 (1990).